PERGAMON International Journal of Multiphase Flow 28 (2002) 1047–1062

International Journal of Multiphase Flow

www.elsevier.com/locate/ijmulflow

Effects of initial bubble size on flow pattern transition in a 28.9 mm diameter column

H. Cheng *, J.H. Hills, B.J. Azzopardi

Department of Chemical Engineering, University of Nottingham, Nottingham NG7 2RD, UK

Received 18 August 1999; received in revised form 8 January 2002

Abstract

The experimental results described in this paper were carried out in a 28.9 mm diameter column at a constant water velocity of 0.356 m/s for four different bubble sizes. The void fraction waves were measured with impedance void fraction meters. It has been found that the initial bubble size has strong effects on the flow pattern transition and the instabilities of void fraction waves. The critical void fraction at which the flow pattern transition happens decreases with increasing bubble size. At a constant liquid velocity with increasing gas flow rate, the point at which the system gain factor becomes larger than 1, and the point where the wave velocity gradient first becomes negative, also decrease with increasing bubble size. This study has confirmed that the instability of the void fraction wave is not the factor that causes the bubble-to-slug flow pattern transition in gas–liquid verticle flow.

Keywords: Instability of void fraction waves; Bubble size effect; Bubble-to-slug flow pattern transition; Gas–liquid two-phase flow

1. Introduction

Bubble flow is characterised by discrete bubbles, which are approximately uniformly distributed in a continuous liquid phase, while slug flow is characterised by Taylor bubbles which have a diameter almost equal to the pipe diameter. These Taylor bubbles move uniformly upward, and are separated by slugs of continuous liquid, which bridge the pipe and may or may not contain small gas bubbles. Between the Taylor bubbles and the wall of the pipe, liquid flows downward in

* Corresponding author. Address: Department of Mechanical Engineering, University of Surrey, Guildford, GU2 5XH, UK.

E-mail address: h.cheng@surrey.ac.uk (H. Cheng).

0301-9322/02/$ - see front matter
PII: S0301-9322(02)00013-7

the form of a thin falling film. Accurately predicting the transition of bubble to slug is critical and important, due to the fact that slug flow may cause undesirable pressure fluctuations, even hammer in pipeline flows; especially severe slugging may pose a threat to safety or undermine the reliability of the system.

Following the work of Radovcich and Moissis (1962), it has been believed that bubbly flow is a transient flow in which bubble coalescence gradually occurs along the channel leading to larger and larger bubbles, and ultimately to slug flow. Given a sufficiently long residence time in a pipe, a swarm of bubbles will develop into slug flow. However, publications on void fraction waves from the Grenoble laboratory (Mercadier et al., 1979; Bouré and Mercadier, 1982; Matuszkiewicz et al., 1987) have challenged the classical picture of bubble-to-slug flow pattern transition, by suggesting that the flow pattern transition is associated with the instabilities of void fraction waves. In addition, Hewitt (1990) studied the bubble–slug transition in a 31.8 mm pipe for different channel lengths, and found that there was no effect of channel length on the transition condition. Wallis (1969) emphasised that wave theory is a very powerful technique for analysing unsteady flow and transient response, and that flow regime changes can be attributed to instabilities which result from wave amplification. The importance of the void fraction wave was not recognised at that time, except for one experimental investigation by Nassos and Bankoff (1966), in which they studied the propagation and amplification of void fraction waves. Publications on this area were very rare until the early 80s.

Mercadier (1981) investigated the propagation of natural void fraction waves in vertical air–water flow in an annulus with mean void fraction ranging from 0 to 0.28, and discovered that the void fraction waves are damped for bubble flow and the damping decreases as the mean void fraction increases. He first put forward the hypothesis that at a certain mean void fraction, the damping could disappear and that the flow pattern transition from bubble to slug could be related to instability of void fraction waves. To prove his hypothesis, Matuszkiewicz et al. (1987) studied natural void fraction disturbances in a vertically upward nitrogen–water flow in a 2×2 cm^2 cross-section column. The void fraction was varied from 0.1 to 0.5 by changing gas flow rate at a single small liquid flow rate of 0.18 m/s. They simultaneously observed a sharp transition and wave instability for void fractions larger than 0.45, and concluded that their experimental results have substantiated the existence of a relationship between the bubble–slug transition and the instability of void fraction waves. Some more recent papers (Bouré, 1988; Saiz-Jabardo and Bouré, 1989; Kytömaa and Brennen, 1991; Monji, 1993; Park et al., 1993) which covered the bubble-to-slug transition also iterated the above point. Here, it is necessary to remark that all these workers studied the propagation of void fraction waves by varying gas flow rate at fixed liquid flow rate over a limited range of flow conditions without considering the bubble size effects. In all these works, the size of the bubbles produced depended on the gas flow rate, that is, they become gradually larger as gas flow rate increased.

Clark and Flemmer (1985) reported that the bubble-to-slug transition is strongly dependent on the method of gas introduction into the liquid stream. Bilicki and Kestin (1988) also observed that, for a given flow condition, the stable flow pattern in a 20 mm diameter tube can be either bubble flow or slug flow, depending merely on the manner of air injection in the mixer. Serizawa and Kataoka (1987) suspected that bubble size might be the key factor, which caused discrepancies in the phase distribution and flow pattern under similar experimental conditions. Song et al. (1995a,b) experimentally investigated the development of bubble flow structure and the propagation prop-

erties of void fraction waves. They systematically varied the bubble size at different fixed flow conditions in both 25 mm (1995a) and 80 mm (1995b) columns. For bubbly flow with large bubble size, the initiation of the instabilities of void fraction waves indicates the development of bubble clustering to form cap bubbles, whereas, for bubbly flow with small bubble size, it means the appearance of Taylor bubbles. Therefore, Song et al. (1995a) concluded that the neutral stability condition of void fraction waves could be used as an indicator for bubble-to-slug flow regime transition for both bubble sizes. To verify that, experiments were carried out in a 28.9 mm air–water column for four different initial bubble sizes. The flow pattern transition was studied at a constant water velocity of 0.356 m/s by changing gas flow rate for each bubble size. If the instability of void fraction wave is the cause of flow pattern transition from bubble to slug, as stated by Matuszkiewicz et al. (1987) and Song et al. (1995a,b), it would be expected that the onset of wave instability coincide with the visual observed flow pattern transition for each of the different bubble sizes.

In this paper, we present experimental measurements conducted in a 28.9 mm diameter column, in an attempt to find out how bubble size affects flow pattern transition and the onset of wave instability.

2. Experimental set-up and instrumentation

The 28.9 mm diameter column is schematically shown in Fig. 1, and described elsewhere (Cheng et al., 1998). The riser, which is constructed in PVC pipe of 28.9 mm internal diameter, is 4.1 m high, while the downcomer consists of one meter of PVC section where the reference electrodes are installed and a section of transparent flexible pipe. A equal-sized bubble generator, first developed by Serizawa et al. (1988) and also utilised by Liu (1991, 1993) and Song et al. (1995a,b), is placed at the base of the riser, so that bubble size can be controlled by varying the jet water flow rate independent of gas and main liquid rates. Because of the pressure requirement, jet water is supplied through a filter from the laboratory mains, whereas the main water flow is circulated from the separation tank through a pump. The excess water introduced through the jet overflows the weir in the separation tank, and exits to drain through a flexible hose. Both main and jet water flows are metered by separate rotameters. The air flow from the laboratory low-pressure mains is also metered by a rotameter, and the superficial gas velocity is corrected to standard condition (1 atmospheric pressure and 0 °C).

The impedance void fraction meter (IVFM), as schematically shown in Fig. 2, is used to measure the void fraction waves in this investigation. It operates on the principle that the bulk electrical impedance of a mixture is usually different from the impedance of each phase, and is a function of void fraction. Each of the IVFM consists of a main sensor, a reference sensor and a signal processor. A main sensor is a pair of quadrant measuring electrodes (20 mm high) sandwiched between two pairs of shielding electrodes (10 mm high) on each side, the gap between the measuring electrodes and the guard electrodes is 1 mm. The reference sensor is a pair of replicate measuring electrodes installed in the downcomer of the system, where only water flows. The signal processor basically works as a Wheatstone bridge. The measuring electrode pair and the reference electrode pair are connected to each arm of the bridge respectively, and the offset voltage of the bridge is due to the difference in resistance between the main sensor and the reference sensor, and varies with the void fraction in the riser. All these quadrant electrodes, made of stainless steel plate

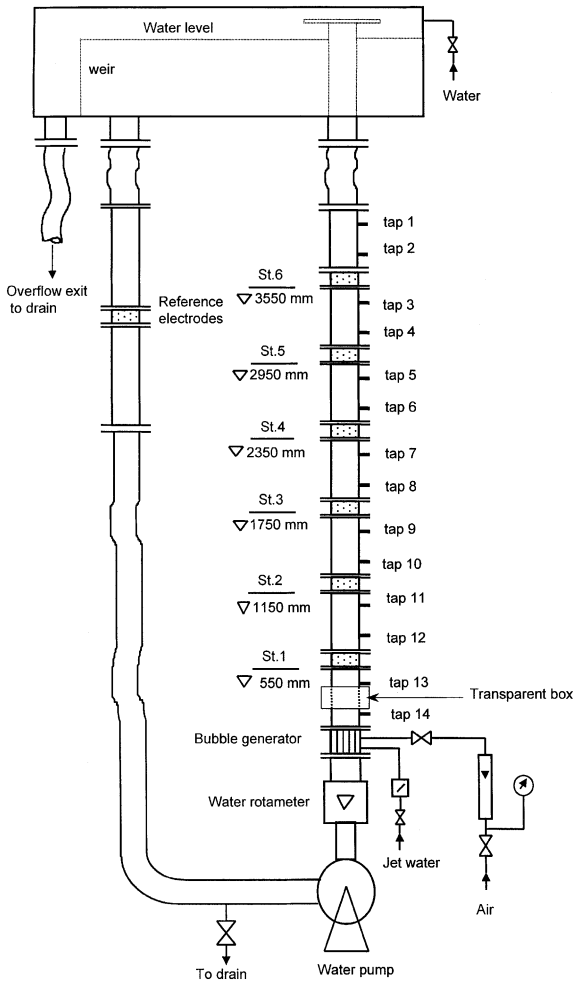

Fig. 1. Experimental rig (ID = 28.9 mm).

with a thickness of 0.076 mm, are flush with the internal wall of the 28.9 mm diameter pipe, to form diametrically opposed 90° arcs on the circumference of the pipe.

Six equally spaced measuring stations are used in this experimental rig with the first station at 0.55 m above the bubble generator. The distance between two successive measuring stations is 0.6 m. There are 14 pressure tappings along the riser at 300 mm intervals, which are connected to manometers. A photographic technique is used to measure initial bubble size at different jet water flow rates. To correct for the channel curvature effect on the sizing, a transparent box filled with water is installed vertically along the column at the bottom of the riser. The box, made of PVC transparent sheet with a thickness of 6 mm, is $10.8 \times 9.4 \times 24.8$ cm and located mid-way between pressure tappings 14 and 13 as shown in Fig. 1.

The calibrations of the IVFMs are conducted in situ at very low liquid flow rates where the pressure drop due to wall friction and liquid acceleration is negligibly small. The output voltage of

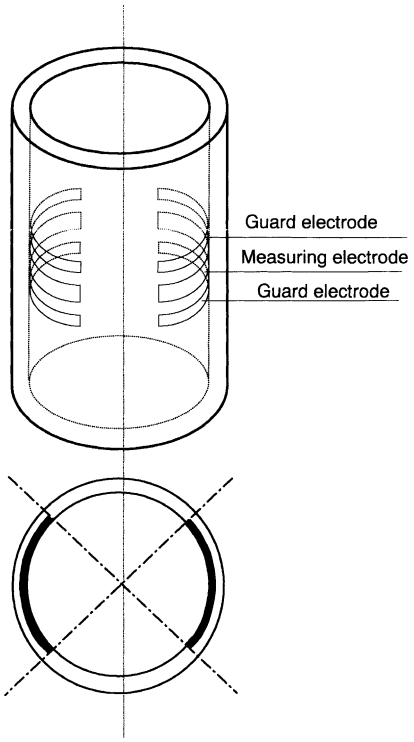

Fig. 2. Impedance void fraction meter.

each IVFM is calibrated against the mean void fraction, which is determined from the pressure drop across the IVFM measured by manometers. The calibration curve, shown in Fig. 3, is empirically fitted by the following equation:

$$V_\varepsilon - V_0 = -0.0127\varepsilon^2 + 0.2158\varepsilon \tag{1}$$

where V_ε and V_0 are the IVFM output voltage of the two-phase flow at void fraction of ε and zero respectively.

The void fraction signals were sampled at 204.8 Hz for 500 s at each location by an A/D card, and analysed by a commercial package called DATS-plus from Prosig.

The initial bubble size controlled by jet water flow rate was determined by analysing the photo image taken by a high-speed video camera at 1000 frames per second. The camera, located at about 250 mm above the bubble generator, is at the same level as the transparent box shown in Fig. 1. At each jet water flow rate, two frames were selected for analysing the bubble size, and on each frame about 20–40 bubbles were captured. A typical photo taken by the high-speed video camera and a processed picture on which the image analysis is based are shown in Fig. 4. The image was analysed by a package called *Optimas 5.1*. The package treats each bubble as an object, and calculates its projected area, perimeter, major axis length (the length of the longest diameter

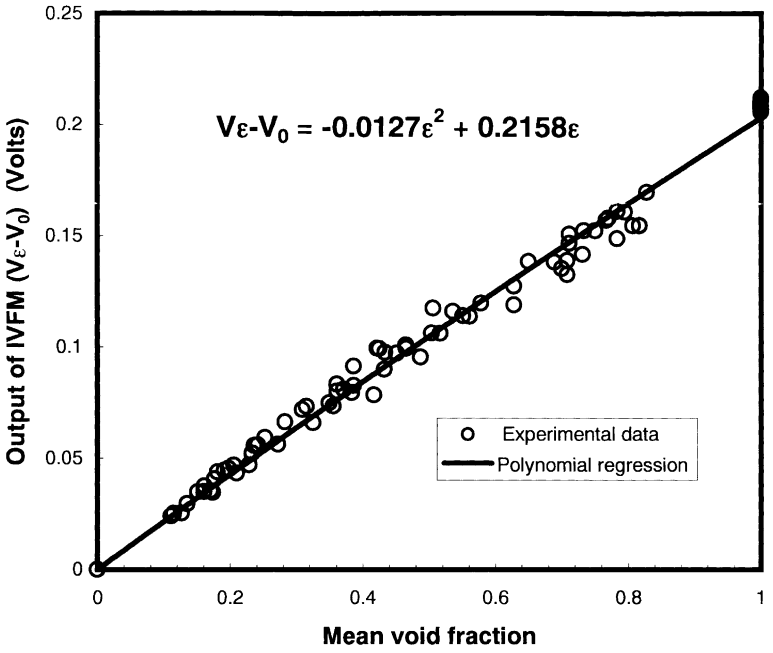

Fig. 3. IVFM calibration curve in the 28.9 mm column.

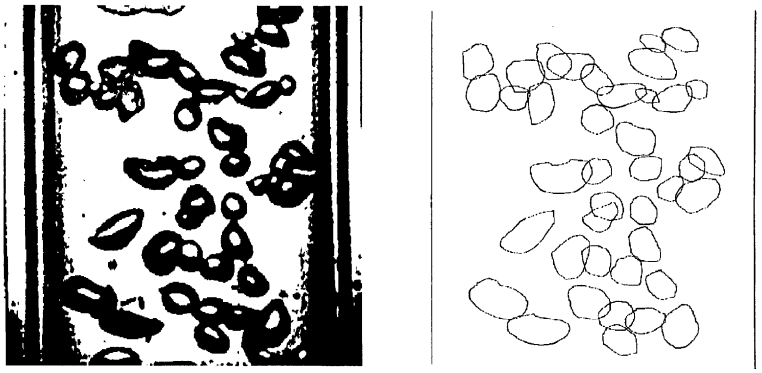

Fig. 4. A typical photo and processed picture for initial bubble size of 3.09 mm.

which may be drawn through the objects), and width (the longest diameter perpendicular to the major axis). The circularity is defined as the ratio of the squared perimeter divided by the area of the object and then divided by 4π, the minimum circularity of 1 is only achieved by a true circle. The mean width over the bubble samples at each jet water flow rate was taken as the mean bubble size for that condition. The characteristics of the bubble size considered in this investigation are summarised in Table 1.

Table 1
Bubble size considered in the present work

No.	Jet water flow rate (l/h)	Mean width (mm)	Mean length (mm)	Mean area (mm^2)	Mean perimeter (mm)	Mean circularity
1	25	4.47	6.37	21.24	17.84	1.25
2	50	3.62	4.91	12.84	13.92	1.23
3	75	3.19	4.31	9.94	12.20	1.22
4	100	3.09	4.50	10.17	12.54	1.27

3. Experimental conditions

The flow pattern transition is studied at a constant water velocity of 0.356 m/s by changing gas flow rate for four different bubble sizes of 4.47, 3.62, 3.19 and 3.09 mm respectively.

For each bubble size, while the liquid flow rate was kept constant, the gas flow rate was gradually increased until the flow pattern was changed from bubble flow to slug flow. At each flow condition, simultaneous measurements were made at successive pairs of the six measuring stations shown in Fig. 1, so that the system gain factor and phase factor of the void fraction signal along the channel can be analysed. For each bubble size, to see if the void fraction wave lost its stability at the condition when the cap bubble flow was observed, the wave growth (or amplification) along the column is analysed for each flow condition, and the onset of the wave instability is compared with the appearance of the cap bubble flow. The detailed flow conditions are listed in Table 2.

4. Data analysis for void fraction waves

From single instantaneous void fraction signals, the probability density function (PDF), the power spectral density function (PSD) and signal-to-noise ratio (SNR) are determined. The PDF and PSD describe the void fraction distribution and the frequency distribution of void fraction waves respectively, the SNR is defined as the standard deviation of the instantaneous void fraction signal normalised by its mean, which reflects the turbulent intensity of the two-phase flow.

From a pair of simultaneous void fraction signals gathered at two successive measuring stations, cross-spectral density function (CSDF) can be estimated. The magnitude and phase of the CSDF yield the system gain factor and phase factor. The phase factor indicates the phase shift between two successive measuring stations for a given wave frequency, from which wave propagating velocity can be obtained. The system gain factor is used to evaluate the degree of wave attenuation or amplification along its propagation path. In this application, the system gain factor represents the ratio of the wave amplitude detected at successive measuring stations. If the system gain factor less than 1, the amplitude of the void fraction wave would become smaller and smaller along its path. If the system gain factor larger than 1, the amplitude of the wave would become larger and larger. Therefore system gain factor equal to 1 is a critical condition which indicates the instability of the void fraction waves. These quantities are used in the sense defined by Bendat and Piersol (1971).

Table 2
Flow conditions

Run no.	Initial bubble size, D_b (mm)	Liquid velocity (m/s)	Gas velocity (m/s)	Mean void fraction at St. 2	Flow pattern
s65	$D_b = 3.09$ mm at $Q_j = 100$ l/h	0.356	0.1315	0.2006	Discrete bubble flow
s15			0.1540	0.2284	Discrete bubble flow
s26			0.1940	0.2786	Cap bubble flow
s27			0.2335	0.3212	Slug flow
s29			0.2978	0.3550	Slug flow
s31			0.3782	0.403	Slug flow
s64	$D_b = 3.19$ mm at $Q_j = 75$ l/h	0.356	0.1319	0.2021	Discrete bubble flow
s14			0.1540	0.2310	Discrete bubble flow
s25			0.1935	0.2753	Cap bubble flow
s28			0.2279	0.3150	Slug flow
s30			0.3017	0.3365	Slug flow
s32			0.3782	0.3816	Slug flow
s67	$D_b = 3.62$ mm at $Q_j = 50$ l/h	0.356	0.0798	0.1296	Discrete bubble flow
s62			0.1315	0.1942	Bubble cluster flow
s13			0.1544	0.2148	Cap bubble flow
s16			0.1897	0.2395	Slug flow
s17			0.2297	0.2736	Slug flow
s20			0.3020	0.3324	Slug flow
s21			0.4984	0.4550	Slug flow
s66	$D_b = 4.47$ mm at $Q_j = 25$ l/h	0.356	0.0616	0.0839	Bubble cluster flow
s68			0.0779	0.1153	Cap bubble flow
s23			0.1308	0.1698	Slug flow
s18			0.2317	0.2606	Slug flow
s19			0.2975	0.3310	Slug flow
s44			0.3797	0.3893	Slug flow
s22			0.5033	0.4628	Slug flow

5. Experimental criteria for the instability of void fraction waves

Many workers have stated that the growth of wave amplitude (i.e. system gain factor larger than 1) along the pipe in the flow direction suggests instability of the void fraction wave (Song et al., 1995a, 1995b; Park et al., 1993), but Matuszkiewicz et al. (1987) pointed out that this cannot be confirmed experimentally in the strict sense, because the growth of the amplitude has to be continued indefinitely for the wave to be unstable. The pipe being of finite length, one cannot be quite sure whether the growth of amplitude is related to an instability of the wave or to a long-

wave phenomenon. However, Whitham (1974) indicated that a continuous wave breaks and becomes unstable if and only if the propagation velocity decreases in the direction of flow. The breaking always appears at some distance from the point where the wave velocity gradient first became negative. In conclusion, the void fraction waves will be experimentally recognised as unstable if amplitude growth and negative wave velocity gradient (deceleration) are simultaneously observed in the column suggested by Matuszkiewicz et al. (1987). In this study, we attempt to establish whether the system gain factor equal to 1 and the wave velocity gradient first becoming negative coincident with the observed flow pattern transition for four different bubble sizes.

6. Results and discussion

6.1. Characteristic PDF for different flow patterns

The classification of the flow pattern was mainly based on visual observations and verified by the PDFs of the void fraction waves. For all the experimental runs, no matter what the initial bubble size is, four typical flow regimes can be identified. Three of them are variations of bubbly flow, and the fourth is slug flow.

6.1.1. Discrete bubble flow

The gas phase is uniformly distributed in the liquid continuum, without bubble agglomeration or coalescence. The time record of this flow shows an apparently random fluctuation with small amplitude, and the PDF shows a single narrow peak as displayed in Fig. 5. It appears at low void fraction for small bubble size.

6.1.2. Bubble cluster flow

In this kind of flow, bubbles agglomerate clump together and consequently form bubble clusters (i.e. void fraction waves). As they travel along the column, the bubble clusters become larger and larger, which is reflected by the broadening of the PDF along the column. The bubble clusters are well indicated in the time record by the void fluctuations with large amplitude. Accompanying the appearance of the bubble clusters, the PDF of the wave signal shows a single peak with a small tail as indicated in Fig. 5. It appears at low void fraction for large bubble size. The discrete bubble flow followed by clustered bubble flow can only occur for intermediate bubble size.

6.1.3. Cap bubble flow

This is a transient region between bubbly and slug flow. For small bubble size, a slight increase in gas flow rate can change the discrete bubble flow into cap bubble flow without obvious clustering. For larger bubble size, as the bubble cluster becomes bigger, some of the bubbles in the cluster coalesce with each other to form a cap bubble. Once cap bubbles are formed, the tailing cap catches up and coalesces with the leading cap, ultimately leading to short slugs. The PDF shows a single peak of bubble flow with a broadening tail extending to higher void fraction as displayed in Fig. 5.

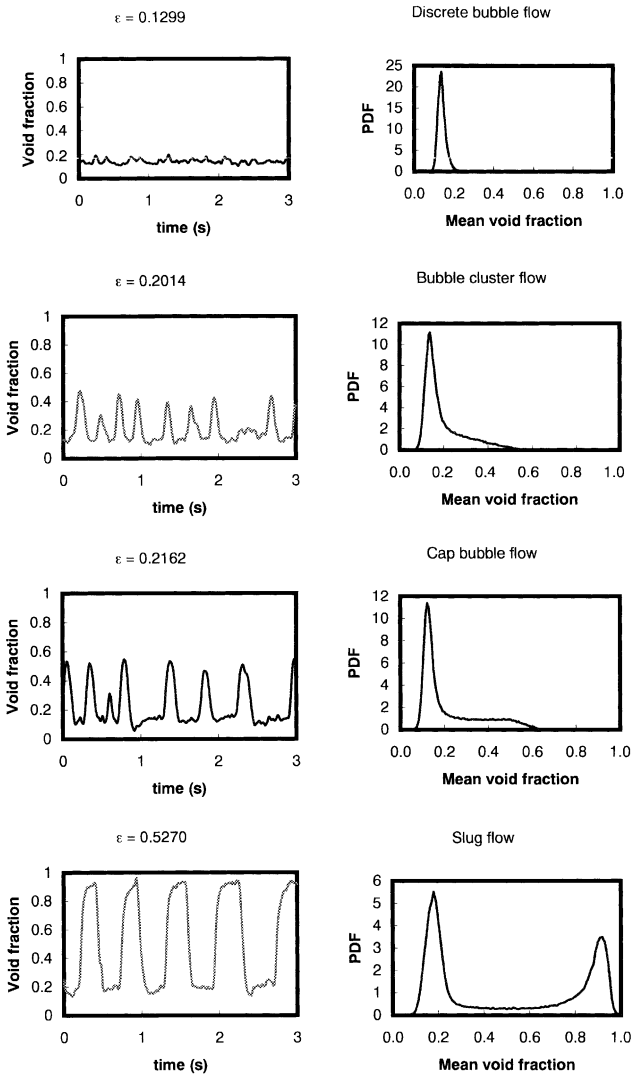

Fig. 5. Typical flow regimes at constant liquid velocity of 0.356 m/s for $D_b = 3.62$ mm (a) discrete bubble flow; (b) bubble cluster flow; (c) cap bubble flow; (d) slug flow.

6.1.4. Slug flow

From cap bubble flow, as the mean void fraction increases further, the flow becomes slug flow, and the slugs are always first observed at the top of the column. A tailing slug travelling in the wake of a leading slug catching up and coalescing to form a larger slug is visually observed, and the tail of the PDF becomes more and more pronounced and eventually develops into a second peak. For developed slug flow, the PDF plot shows twin peaks as demonstrated in Fig. 5, where one represents the void fraction in the liquid slug and the other represents the void fraction in the gas slug.

The PDF of the void fraction waves shows a single peak for bubble flow and double peaks for slug flow, which is in good agreement with the findings of Costigan and Whalley (1997) and many others.

6.2. Effects of bubble size on the instability of the void fraction wave

The variations of system gain factor with mean void fraction along the column during the bubble-to-slug flow pattern transition for four different initial bubble sizes are presented in Fig. 6. These results show that the mean void fraction at which the system gain factor becomes larger

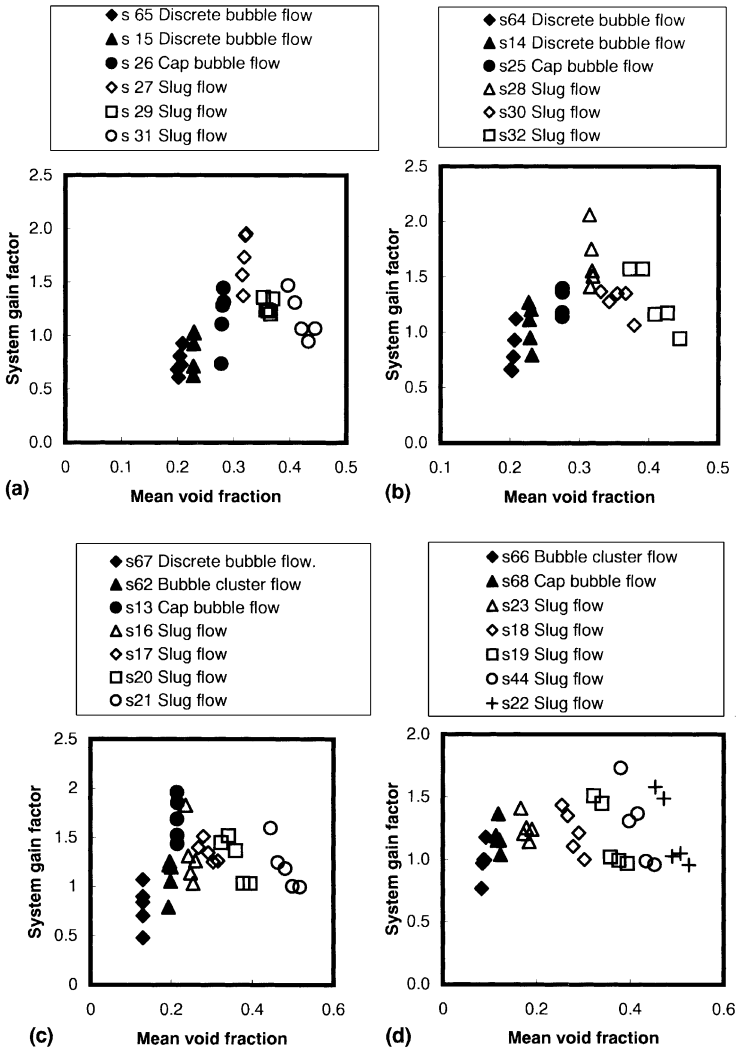

Fig. 6. Variation of system gain factor with mean void fraction at constant liquid velocity of 0.356 m/s in ID = 28.9 mm column for bubble size of (a) 3.09 mm; (b) 3.19 mm; (c) 3.62 mm; (d) 4.47 mm.

than 1 decreases with increasing initial bubble size, in other words, wave growth starts earlier (i.e. at lower gas flow rate) for larger bubble size at the same constant water velocity. The flow condition at which the system gain factor becomes larger than 1 does not coincide in all cases with the condition at which cap bubble flow was observed. The gain factor becomes larger than 1 even for discrete bubble flow and clustered bubble flow with the intermediate and larger bubble sizes, which indicates that the wave growth is closely related to the initial bubble size. Examining the data for all different bubble sizes, it is interesting to note that the gain factor increases up the column for bubbly flows, and decreases up the column for slug flows.

The development of SNR with void fraction along the column for the same flow conditions is shown in Fig. 7. The SNR is very low for discrete bubble flow, and the rapid increase first occurs in cap bubble flow for small bubble size where clustered bubble flow does not exist, or in clustered

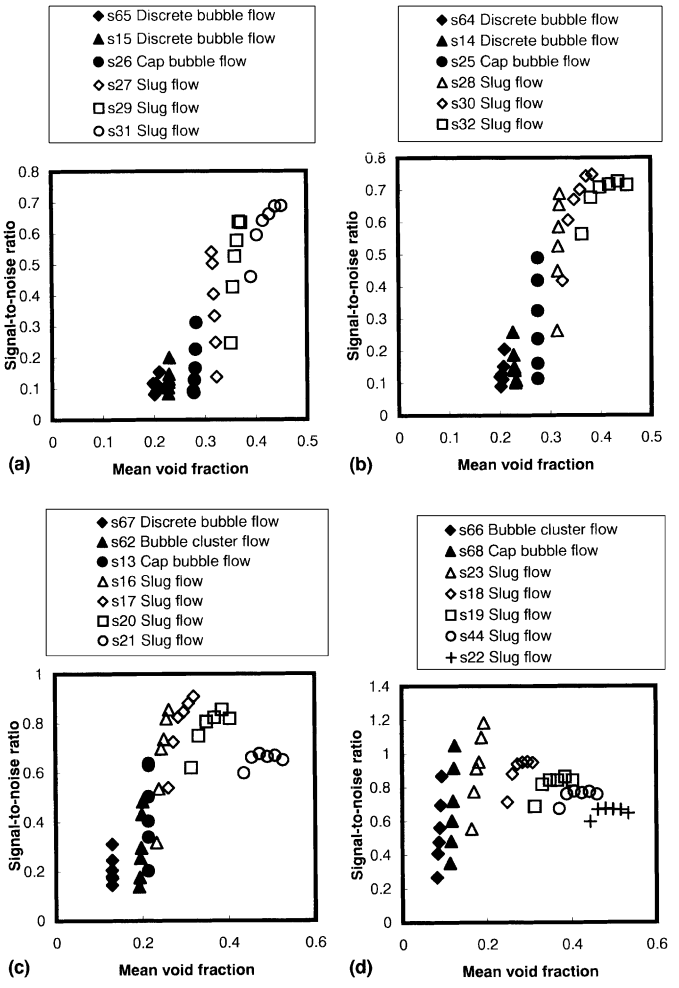

Fig. 7. Variation of signal-to-noise ratio with mean void fraction at constant liquid velocity of 0.356 m/s in ID = 28.9 mm column for bubble size of (a) 3.09 mm; (b) 3.19 mm; (c) 3.62 mm; (d) 4.47 mm.

bubble flow for larger bubble size where discrete bubble flow does not exist. For the four bubble sizes investigated here, the conditions at which the rapid increase in SNR occurs are close to the conditions where cap bubble flow was first observed. These results indicate that the SNR of the void fraction wave is also associated with initial bubble size.

The development of wave velocity for the dominant frequencies along the column at the same experimental conditions is displayed in Fig. 8, the dominant frequency shown in the legends of Fig. 8 is the peak frequency in the PSD curves. When the flow pattern transition is approached at a constant water velocity by increasing gas flow rate, the consistent negative wave velocity gradient was first encountered in run s31 which is slug flow with void fraction of 0.403 for the

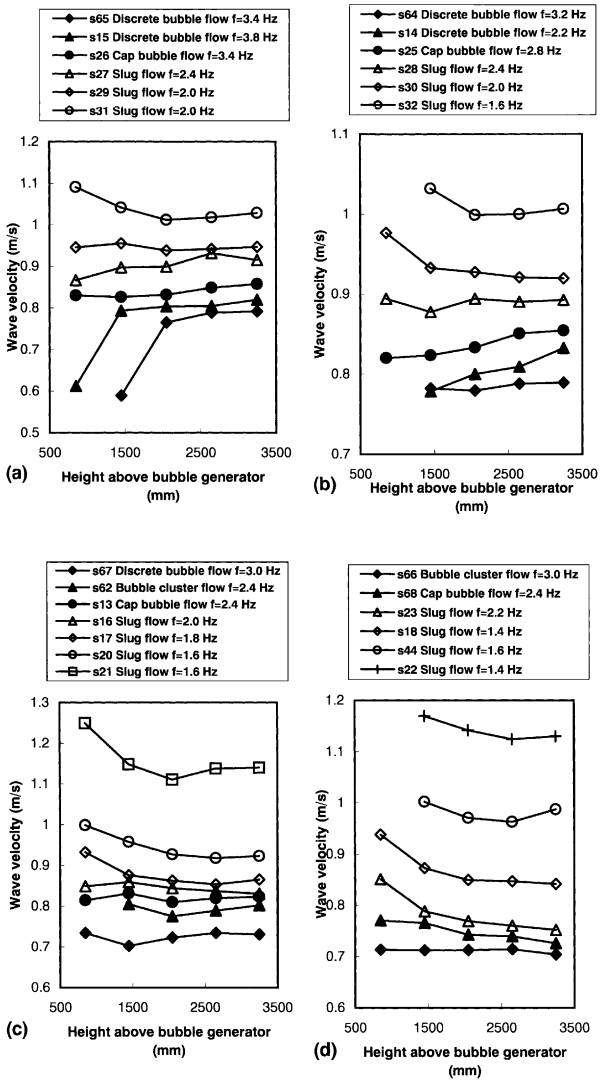

Fig. 8. Wave velocity of dominant frequency against column height constant liquid velocity of 0.356 m/s in ID = 28.9 mm column for bubble size of (a) 3.09 mm; (b) 3.19 mm; (c) 3.62 mm; (d) 4.47 mm.

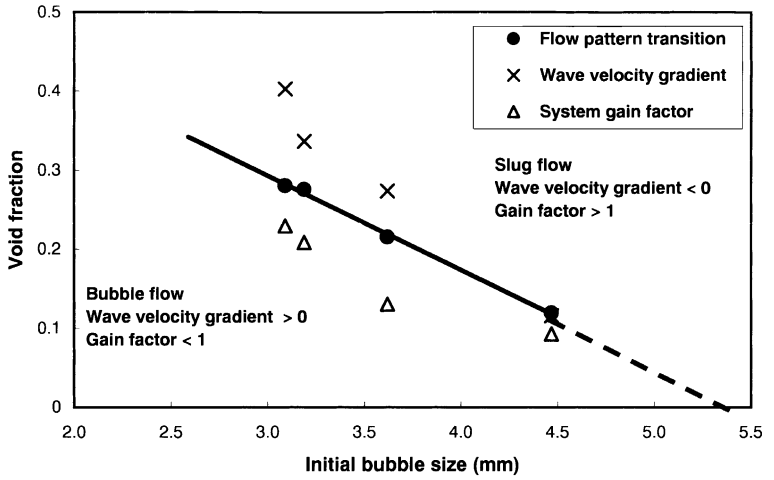

Fig. 9. Critical void fraction against initial bubble size at constant liquid velocity of 0.356 m/s in the ID = 28.9 mm column.

3.09 mm bubbles, run s30 which is slug flow with void fraction of 0.3365 for the 3.19 mm bubbles, run s17 which is also slug flow with void fraction of 0.2736 for the 3.62 mm bubbles, and run s68 which is cap bubble flow with void fraction of 0.1153 for the 4.47 mm bubbles. These conditions are not coincident with the observed flow pattern transition in the column except for bubble size of 4.47 mm. It is clear that the onset of negative wave velocity gradient is also affected by the initial bubble size, the wave gradient first becomes negative at higher void fraction for smaller bubble size. As mentioned earlier, the slugs are first observed at the top of the column, the data in Fig. 8 clearly shows that the negative wave gradient first appears at the bottom of the column, which is another indication that the two phenomena are not closely linked. The void fraction at which the system gain factor first becomes larger than 1, and the void fraction at which the wave velocity first becomes negative, are plotted against initial bubble size in Fig. 9.

6.3. Effects of bubble size on the flow pattern transition of bubble to slug

Based on the visual observations at a constant water flow rate listed in Table 2, it is found that the cap bubble flow was observed at different gas flow rates for different bubble sizes. The critical void fraction at which cap bubble flow was first observed is also plotted against bubble size in Fig. 9. It seems that a straight line can be drawn between the border of bubble flow and slug flow. If this boundary line is extrapolated, it crosses the horizontal axis at about 5.46 mm. This suggests that bubbly flow may disappear completely in this column if the initial bubble size is larger than 5.46 mm. This in a sense supports the theory proposed by Taitel et al. (1980), in which they predicted a steady bubble flow could not exist in tubes with diameter less than 50 mm, but they did not consider the bubble size effect. The critical void fraction at which the flow pattern transition of bubble to slug occurs decreases with increasing initial bubble size, which has confirmed the results by Song et al. (1995a,b) who studied the bubble size effect on flow pattern transition in both 80 and 25 mm columns. As a practical implication, in order to avoid the undesirable pressure

fluctuations introduced by slug flow, the hole in the gas generator should be fine when producing gas–liquid two-phase flows in narrow tubes.

As also demonstrated in Fig. 9, the point at which the system gain factor became larger than 1, and the point where the wave velocity gradient first became negative, do not coincide with each other nor with the visually observed flow pattern transition for bubble sizes less than 4.47 mm. The three transitions appear to get close together at large bubble size. The system gain factor becomes larger than 1 before the transition, and the wave velocity gradient first becomes negative after the flow pattern transition. These results also confirm that the instability of void fraction waves is not the factor, which causes the flow pattern transition to happen as has been suggested in the literature by many recent investigators, such as Matuszkiewicz et al. (1987) and Song et al. (1995a,b).

7. Conclusions

During the bubble-to-slug flow pattern transition, the investigation into the instability of the void fraction waves in the 28.9 mm diameter column for four different bubble sizes has led to the following conclusions:

(1) Initial bubble size has strong effects on the flow pattern transition. The critical void fraction at which the flow pattern transition happens decreases with increasing initial bubble size.

(2) Bubble size also affects the instability of void fraction waves. At constant liquid velocity with increasing gas flow rate, the conditions at which the system gain factor equals to 1, and the conditions at which the wave velocity gradient first becomes negative, also decrease with increasing bubble size. However, these effects do not happen simultaneously, nor are they coincident with the visual observations of flow pattern transition in the column except for one bubble size.

(3) At fixed gas and liquid flow conditions, the flow pattern can be either bubble flow or slug flow strongly depending on the initial bubble size. Therefore, any theoretical model, which was used to predict the bubble-to-slug flow pattern transition without considering the bubble size, would be unreliable.

Acknowledgements

This research was sponsored by EPSRC under a research grant no. GR/J47392, whose financial support is gratefully acknowledged. We wish to thank Dr. E. Lester for his help in analysing the photo image for the bubble sizes, and we are grateful to the referees for carefully reading the manuscript and making interesting comments.

References

Bendat, J.S., Piersol, A.G., 1971. Random Data: Analysis and Measurement Procedures. Wiley-interscience, New York.

Bilicki, Z., Kestin, J., 1988. Experimental investigation of certain aspects of upward vertical bubble and slug flows. Exp. Fluids 6, 455–460.

Bouré, J.A., Mercadier, Y., 1982. Existence and properties of flow structure waves in two-phase bubbly flow. In: Van Wijingaarden, L. (Ed.), Applied Scientific Research, Mechanics and Physics of Bubble in Liquid, vol. 38, pp. 297–303.

Bouré, J.A., 1988. Properties of kinematic waves in two-phase pipe flow consequences on the modelling strategy. European Two-Phase Flow Group Meeting, Brussels, 30 May–1st June.

Cheng, H., Hills, J.H., Azzopardi, B.J., 1998. A study of the bubble-to-slug transition in vertical gas–liquid flow in columns of different diameter. Int. J. Multiphase Flow 24, 431–452.

Clark, N.N., Flemmer, R.L.C., 1985. The bubble to slug flow transition in gas–liquid upflow and downflow. J. Pipelines 5, 53–65.

Costigan, G., Whalley, P.B., 1997. Slug flow regime identification from dynamic void fraction measurements in vertical air–water flows. Int. J. Multiphase Flow 23, 263–282.

Hewitt, G.F., 1990. Non-equilibrium two-phase flow. In: Proceedings of the 9th International Heat Transfer Conference, Jerusalem, Israel, vol. 1, pp. 383–394.

Kytömaa, H.K., Brennen, C.E., 1991. Small amplitude kinematic wave propagation in two-component media. Int. J. Multiphase Flow 17, 13–26.

Liu, T.J., 1991. The effect of bubble size on void fraction distribution in a vertical channel. In: Proceedings of the International Conference Multiphase Flows'91-Tsukuba, September 24–27, 1991, Tsukuba, Japan, pp. 453–457.

Liu, T.J., 1993. Bubble size and entrance length effects on void development in a vertical channel. Int. J. Multiphase Flow 19 (1), 99–113.

Matuszkiewicz, A., Flamand, J.C., Bouré, J.A., 1987. The bubble–slug flow pattern transition and instabilities of void fraction waves. Int. J. Multiphase Flow 13 (2), 199–217.

Mercadier, Y., Van Schaik, J.C.H., Bouré, J.A., 1979. Experimental analysis of void fraction disturbances in a nitrogen–water bubbly flow. European Two-phase Flow Group Meeting, Ispra.

Mercadier, Y., 1981. Contribution à l'é tude des propagations de perturbation de taux de vide dans les écoulements diphasiques eau-air à bulles. Thèsis, Université Scientifique et Médicale et Institut National Polytechnique de Grenoble, France.

Monji, H., 1993. Transition mechanism from bubble flow to slug flow in a riser. Fluid Dyn. Res. 11, 61–74.

Nassos, G.P., Bankoff, S.G., 1966. Propagation of density disturbances in an air–water flow, AIChE, In: Proceedings of the Third International Heat Transfer Conference, 7–12 August, Edgewater Beach Hotel, Chicago, Illinois, vol. IV, pp. 234-246.

Park, J.W., Lahey Jr., R.T., Drew, D.A., 1993. The measurement of void waves in bubbly two-phase flows. In: Proceedings of the 6th International Meeting Nuclear Reactor Thermal-Hydraulics, Grenoble, 5–8 October 1993, pp. 655–662.

Saiz-Jabardo, J.M., Bouré, J.A., 1989. Experiments on void fraction waves. Int. J. Multiphase Flow 15 (4), 483–493.

Serizawa, A., Kataoka, I., 1987. Phase distribution in two-phase flow. In: Proceedings of the Transient Phenomena Multiphase Flow, ICHMT, Int. Seminar, Dubrovnik, Croatia, pp. 179–224.

Serizawa, A., Kataoka, I., Zun, I., Michiyoshi, I., 1988. Bubble size effect on phase distribution. In: Proceedings of the Japan-US Seminar Two-Phase Flow Dynamics, pp. 15–20.

Song, C.H., No, H.C., Chung, M.K., 1995a. Investigation of bubble flow developments and its transition based on the instability of void fraction waves. Int. J. Multiphase Flow 21, 381–404.

Song, C.H., Chung, M.K., No, H.C., 1995b. The effect of bubble flow structures on the void wave propagation in a large diameter pipe. In: Proceedings of the 2nd International Conference Multiphase Flow'95, 3–7 April 1995, Kyoto, Japan.

Taitel, Y., Barnea, D., Dukler, A.E., 1980. Modelling flow pattern transition for steady upward gas–liquid flow in vertical tubes. AIChE J. 26, 345–353.

Radovcich, N.A., Moissis, R., 1962. The transition from two-phase bubble flow to slug flow. MIT Report No. 7-7673-22.

Wallis, B., 1969. One-dimensional two-phase flow. McGraw-Hill, New York.

Whitham, G.B., 1974. In: Linear and Non-linear Waves. Wiley-interscience publication, John Wiley and sons, New York, p. 37.